

Fracture mechanism and separation conditions of pineapple fruit-stem and calibration of physical characteristic parameters

Mutong Li^{1*}, Lin He¹, Dandan Yue², Binbin Wang¹, Junlue Li¹

(1. Key Laboratory of Modern Agricultural Intelligent Equipment in South China, Ministry of Agriculture and Rural Affairs of China, Guangdong Institute of Modern Agricultural Equipment, Guangzhou 510630, China;
2. Guangdong Hongke Agricultural Machinery Research and Development Co., Ltd, Guangzhou 510555, China)

Abstract: At present, the research on the physical composition and properties of pineapple plants is scarce, and the uncertainty of fruit picking method is the key bottleneck factor hindering the research and development of pineapple harvesting machinery. Based on the statistics of survey data from many places, this paper analyzes the fruit-stem fracture mechanism and the theoretical conditions for optimal separation through structural modeling, mechanical behavior analysis and function judgment. On this basis, the “pineapple plant fixation bench” and “fruit-stem bending separation torque test equipment” were developed, and large-size, small-size tests and random optimization tests were carried out successively. The test results showed that the larger of the stem-stalk fixation distance, the more torque and fracture starting angle required for fruit fracture would increase, and the change range was small when the stem-stalk fixation distance was within 50 mm, and the probability of brittle fracture and complete separation was very high. When the space between the fracture section and the fruit-stem connecting point is about 5mm, the range of bending moment value required for the fruit-stem fracture is 1.88 to 2.77 N·m, the range of fracture starting angle is 12.2° to 18.1°, and the angular travel range during the separation process is 82.9° to 87.5°. When the stem-stalk fixation distance is about 15 mm, it is the best fruit-stem separation condition and the breaking torque measured in the verification test is about 2.76 N·m. The fracture starting angle is about 13.8°, the maximum prediction error is 13.1%, and the elastic modulus near the fruit-stem joint ranges from 16.1 to 23.9 MPa. This conclusion can provide an important design basis for the research and development of pineapple field picking robot and harvesting equipment.

Keywords: pineapple harvesting, fracture mechanism of fruit and stem, separation conditions, experiment design, reverse calibration

DOI: [10.25165/j.ijabe.20231605.8079](https://doi.org/10.25165/j.ijabe.20231605.8079)

Citation: Li M T, He L, Yue D D, Wang B B, Li J L. Fracture mechanism and separation conditions of pineapple fruit-stem and calibration of physical characteristic parameters. *Int J Agric & Biol Eng*, 2023; 16(5): 248–259.

1 Introduction

The pineapple planting area in China is about 1 million mu, and the output is about 1.8 million tons, accounting for about 7% of the that in the world. Among them, the output of Guangdong Province and Hainan Province accounts for 90% of the national total output. In recent years, with the improvement and optimization of species, the planting area is also increasing year by year. However, the lack of pineapple picking and harvesting equipment has led to low efficiency of traditional harvesting and high labor cost^[1], which has caused the imbalance between supply and demand in the pineapple industry, led to the sharp price decline and fluctuation and dull sale. The fundamental reason for its “machine unavailability” is the lack of the basic research of the R&D personnel on the fruit-stem separation mechanism and fracture behavior, and the insufficiency

of integration of agronomy and agricultural machinery. Therefore, the research on the physical and mechanical properties of pineapple plants has become an urgent priority at present. It is also an important theoretical support and design basis for the success of the development of harvesting equipment^[2,3].

Up to now, most pineapples are planted in Costa Rica, Brazil, the Philippines, Thailand, and Indonesia^[4,5]. Less attention was paid to the scientific research on pineapple harvesting technology and crop mechanics. Therefore, the related research results are less^[6,7]. In recent years, only a few colleges and universities in China have preliminarily carried out some exploratory research. For example, Liu et al.^[8,9] applied vertical pressure to different positions of the fruit and stem after fixing the pineapple plant in the horizontal direction, tested the breaking moment of the calyx separation layer, and then designed a flexible finger roller harvesting device. However, the roots of pineapple plants in the field are fixation into an upright cantilever structure, the fruit mass accounts for a large proportion and grows on the top of the plant. The crushing test results after “horizontal” fixation are greatly affected by gravity. At the same time, the test results of the root in a free state can no longer accurately reflect the stress and deformation of the stem in the process of fruit fracture; Li et al.^[10] designed a plant fixation test bench for simulating the growth posture of pineapple in the field and a recyclable split pineapple plant monomer model, which solved the problems of long cycle, difficulty and slow harvest test of field pineapple planting, and created an indoor all-weather harvest test platform. But it only provided a functional test carrier,

Received date: 2022-12-16 **Accepted date:** 2023-06-29

Biographies: **Lin He**, MBA, research interest: design of agricultural machinery in hilly and mountainous areas, Email: 75318013@qq.com; **Dandan Yue**, Master, research interest: design and experimental research of agricultural machinery, Email: 1060260663@qq.com; **Binbin Wang**, Bachelor, research interest: harvester design and manufacturing, Email: beenwong@163.com; **Junlue Li**, MBA, research interest: planning of agricultural machinery and equipment in South China, Email: lijunlue@188.com.

***Corresponding author:** **Mutong Li**, PhD, Senior Engineer, research interest: reliability technology of agricultural machinery in hilly area, and the key technologies of pineapple picking and harvesting. Guangdong Institute of Modern Agricultural Equipment, Guangzhou 510630, China. Tel: +86-18312222400, Email: 236280045@qq.com.

because the difference of physical characteristics between the model and the real object needs to be tested and corrected; Zhang et al.^[11,12] developed an automatic pineapple picker. However, since the bottom of the pineapple fruit is often accompanied by delicate bud supporting seedlings, an important seedling for the next round of transplanting. If cutting, it is very easy to cause seedling damage when using rolling or rigid roller to forcibly separate the fruit, which violates the agronomic requirements for seedling cultivation, and the technical route needs to be adjusted. At present, fruit harvesting can only be achieved by grasping the upper end of the fruit and pressing or bending it toward one end. Therefore, in order to study the fracture and separation of pineapple fruit stem, plant monomer needs to be taken as the research object to analyze the changes of shape, size and mechanical behavior during the process of external force, and then accurately grasp the separation mechanism.

To sum up, at present, the basic research on pineapple fruit stem/stem fracture mechanism and separation conditions is less, and it is urgent to obtain more accurate conclusions through targeted design and test, which can lay the necessary design basis and

theoretical support for the development of pineapple harvesting equipment^[13-15]. This study will take the field harvest method of pineapple fruit as the premise to study the fracture and separation mode of fruit and stem. Through the self-developed torque measurement test equipment for fruit stem fracture separation, the twist test research of pineapple fruit will be carried out. With the fixation height between stem and stalk as the variable factor, the fracture limit torque and the fracture angle of fruit as the indicators, the fracture mechanical behavior test research will be carried out to clarify the optimal separation conditions of fruit and stem. According to the test results, the parameters of physical properties are calibrated to grasp the optimal conditions of fruit harvesting and guide the design of key components and core devices of harvesting equipment. Therefore, it is necessary to clarify the growth mode at first, basic size parameters and structural characteristics of pineapple plants in the field, and then build a reasonable model, so as to lay a foundation for the experimental study of physical and mechanical properties. The overall technical roadmap of this study is shown in Figure 1.

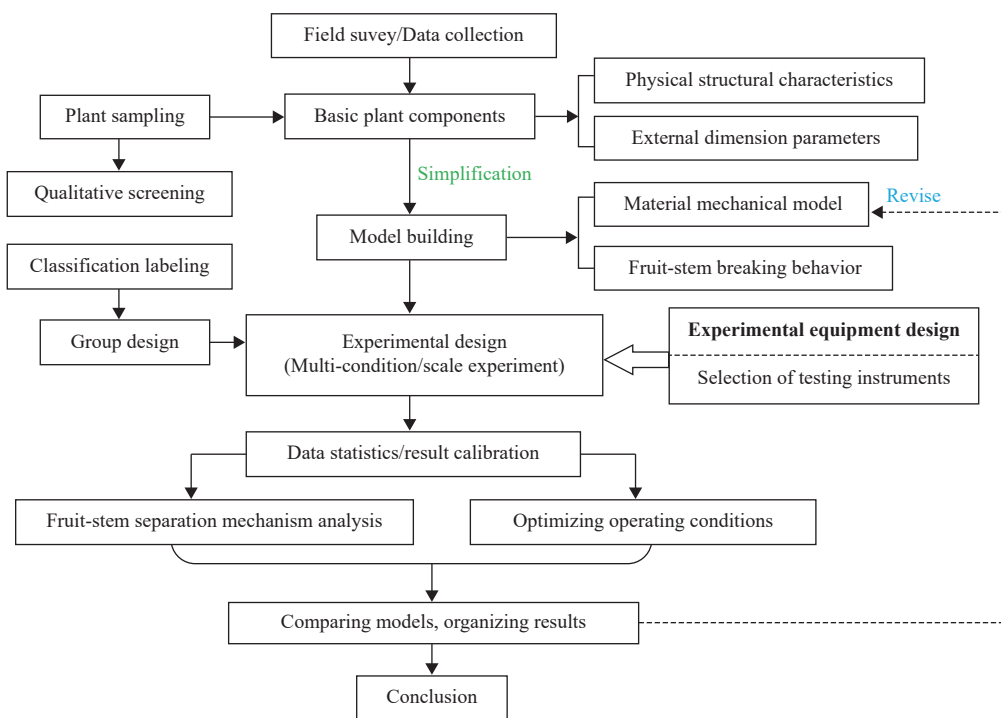


Figure 1 Research roadmap diagram

2 Materials and methods

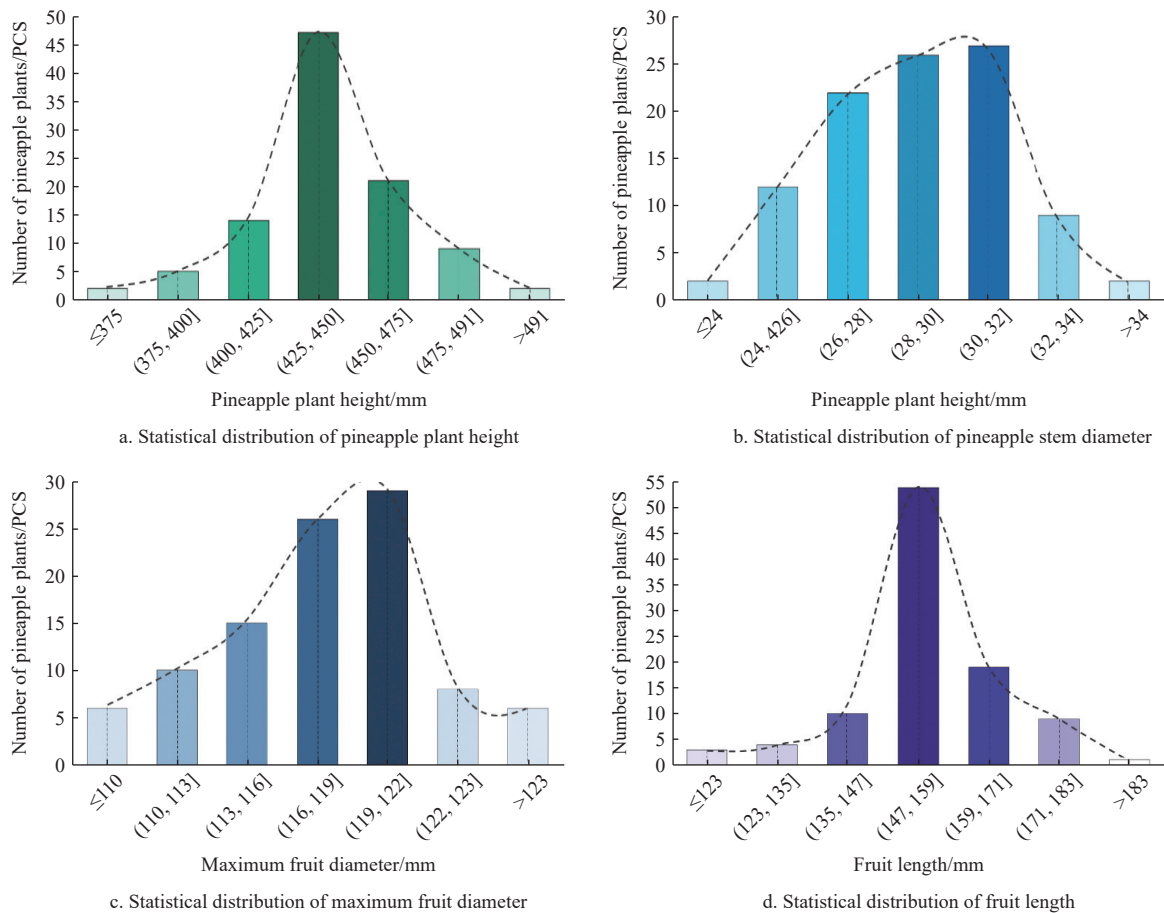
2.1 Basic composition and physical characteristics of plant

Compared with other fruits, the separation method of pineapple fruit and stem is relatively simple. The connection area between the calyx at the bottom of the fruit and the fruit stalk at the top of the stem is mainly composed of brittle structures. Generally, after the fruit is gripped and fixation, it can be easily broken completely by pressing in one direction, and there is no attachment and entanglement of fibrous filament structures at the fracture^[16,17]. Therefore, The growth mode of pineapple plant has better conditions for fruit stem separation test. However, two kinds of forces are mainly involved in the process of fruit “breaking”. One is the resultant force of rebound bending moment caused by certain bending deformation of the stem when the fruit is pressed, and the other is the partial shear force generated at the section of the fruit

stem connection. The difficulty of breaking is also affected by many factors such as fruit maturity, variety, plant height and material properties^[18,19].

2.1.1 Measurement of external dimension parameters

In May 2022, field investigation and sample collection were carried out in Qujie Town, Xuwen County, Zhanjiang City, Guangdong Province, China (20°29'24.66"N, 110°19'18.83"E). 100 varieties of Bali with maturity of C0-C2 were selected as the measurement objects^[20], and their plant height, straight diameter of stem, maximum diameter of fruit and length of fruit were measured. The results are shown in Figures 2a-2d. The overall results are approximate to normal distribution. The most plant height ranges from 425 to 450 mm, the stem diameter ranges from 26 to 32 mm, the maximum fruit diameter ranges from 116 to 122 mm, and the fruit length ranges from 147 to 159 mm.



*Note: Generally, plants with good verticality are selected for the measurement of plant height, and the distance between the fruit stem connection and the soil contact point at the bottom of the stem is measured; For the measurement of stem diameter, this paper selects three positions of stem, namely, high position, middle position and low position, to measure and record the mean value.

Figure 2 Histogram of external size statistics of pineapple plant

2.1.2 Crop structure and characteristics

The root system of pineapple plant is fibrous root, which is mostly distributed in the depth of 100~250 mm below the soil. Generally, after the fruit enters the mature period (can be harvested), there are lush and serrated leaves around the stem, and often accompanied by a variety of bud seedlings, as shown in Figure 3a. Among them, offsets (also known as supporting buds) and seed buds (also known as leaf buds) are the main seedlings used for the next round of transplanting. In addition, plants with sprouts need to be left in the field for about four months after fruit harvesting. Generally, in order to avoid damaging stems or sprouts during fruit harvesting, forced feeding, cutting, or pulling stems are not used for harvesting.

2.2 Mechanism of bending separation and fracture

2.2.1 Mechanical behavior analysis

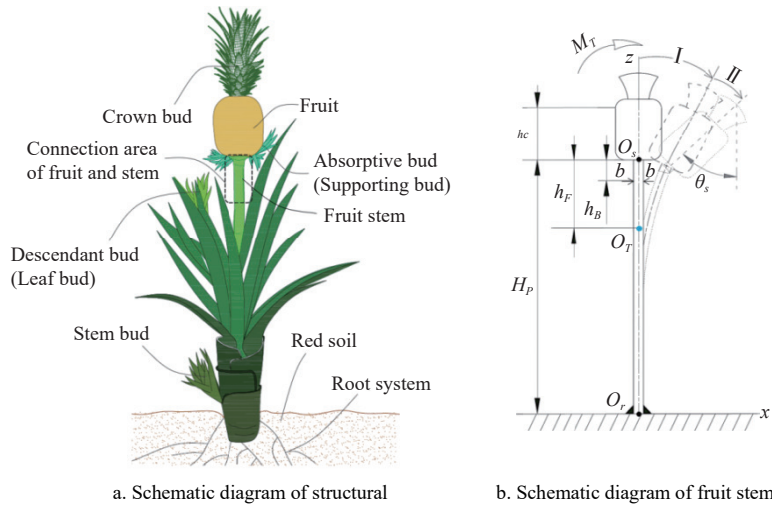
As shown in Figure 3b, the plant monomer is abstracted as a rigid body, and its stem is a fleshy near spindle like cylinder, so it is regarded as a vertical cantilever beam structure of a variable cross-section rod. The lower grounding root is a fixation end, and the connection area between fruit and crown is a free end (ignoring the part of crown leaf of the fruit crown). When the fruit is subjected to external forces, the whole fracture process of the separation of fruit and stem can be disassembled into two stages. The first stage is the elastic deformation process of the stem, in this stage, the root is used as the fixation end to provide the reaction force, and the stem will overcome the bending stiffness and have a certain flexible deformation, and will be in a critical equilibrium state after reaching the maximum angle. The second stage is the process of destructive

fruit-stem fracture. In this stage, there are many bud differentiation points and dormancy points in the stems near the junction of fruit and stem (also called calyx or fruit stalk). The section of the stems subjected to external forces is subject to bending moment and shear at the same time. When the material strength limit is reached, fracture will occur somewhere.

However, the above analysis on the process of fracture of fruit and stem mainly carried out disassembling basic action in the way of magnifying mechanical. Taking the grounding root as the constraint center point, applying a constant force in the straight direction to the fruit will produce greater stem deformation, and the time consumption for fracture and separation will also be lengthened. In the actual field harvest, in order to ensure rapid and efficient separation of fruit and stem, usually, supporting points corresponding to O_T in Figure 3b, also known as auxiliary constraint points, are added to the stem at a certain height, and pineapple fruit is bent with the bending moment center near the supporting point, reducing the deformation deflection of the stem at the first stage, saving the time and space for separation of fruit and stem. To sum up, it is necessary to further build a fruit-stem mechanical model in pineapple plants, so as to obtain the main factors affecting fruit separation more scientifically through experiments.

2.2.2 Mechanical behavior analysis

As shown in Figure 3b, during actual fracture, the fixed end will be replaced by the external auxiliary constraint point O_T in the natural state O_r point. After fixed clamping somewhere on the surface of the fruit, the approximate O_T point is taken as the center of rotation, and the fruit is uniformly twisted clockwise until it

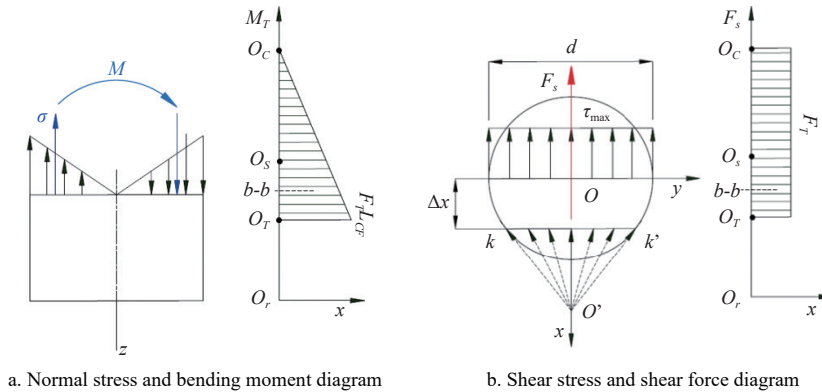


*Note: O_r in the figure is the stalk grounding point and also the constraint point of the vertical cantilever model. O_s is the connection point of fruit and stem(also known as the calyx and connection point of fruit and stalk), which is artificially defined for the convenience of measurement, specifically the junction between the bottom of the fruit and the top of the stem. H_p is the plant height, that is, the distance between O_r and O_s , mm; h_c is the clamping height of fruit and stem (also known as the grasping height or the fixation fruit height), that is, the distance between the fruit clamping point and O_s , which is the test variable factor, mm; The auxiliary restraint point between O_r and stem is also the rotation center point of fruit torsion test; h_f is the fixation space between stem and stalk, that is, the space between O_r and O_s , and is the test variable factor, mm; h_b is the breaking distance, is the distance between the fruit-stem breaking point and O_s , is the test result to be measured, mm; $b-b$ is the fruit-stem fracture section; I is the process of pineapple plant from natural state to elastic deformation state under the action of external force, which is defined as the first stage in this paper; II refers to the process of stem from critical equilibrium to fruit stem fracture, which is defined as the second stage in this paper; θ_s is the fruit fracture angle, that is, the angle between the fruit axis and the vertical direction at the critical moment of fruit stem separation, ($^\circ$); M_r is the torque acting on the fruit, N·m.

Figure 3 Composition and mechanical model of pineapple plant

breaks. It can be seen from Figure 4 that the fruit and stem are approximately regarded as two cylindrical beams of equal section with different diameters. During the bending and breaking process, the maximum section of bending moment is around the O_r point of the center of rotation, and the shear force is evenly distributed at each point. Because the stem is different from the rigid beam of uniform material, it cannot be directly defined as plastic or brittle

material, and both the normal and shear stresses can lead to fracture. And it may occur at the section with the maximum bending moment, or at the section diameter mutation (that is, fruit-stalk junction).Therefore, it is assumed that $b-b$ is a fracture section at any place between O_s and O_r , the maximum normal stress σ_{bmax} and maximum shear stress τ_{bmax} in the instantaneous critical state of fracture shall meet the following conditions.



*Note: $k-k'$ in the figure refers to the section chord passing through the section center arbitrarily; Δx is the translation of the chord section with the neutral axis (diameter); For circular section beams, according to the reciprocal theorem of shear stress, the direction of shear stress at each point on the section edge is tangent to the circumference, and the shear stress at each point on the neutral axis is maximum; O_c is the action point of external bending moment of pineapple fruit.

Figure 4 Internal force distribution on the overall section of plant

$$[\sigma_{bmax} \geq \sigma_\mu] \vee [\tau_{bmax} \geq \tau_\mu] \tag{1}$$

where, σ_μ is ultimate normal stress of straw material, MPa; τ_μ is shear strength limit of straw material, MPa.

The calculation basis of normal stress σ_b (MPa) and shear stress τ_b (MPa) at section $b-b$ is

$$\begin{cases} \sigma_b = \frac{M_b}{W_z} = \frac{M_b}{\pi d^3/32} \approx \frac{M_b}{0.1d^3} \\ \tau_b = \frac{F_s S_z^*}{I_z d} = \frac{F_s d^3/12}{(\pi d^4/64)d} = \frac{16F_s}{3\pi d^2} \end{cases} \tag{2}$$

where, M_b is bending moment required for fracture of section $b-b$, N·m; W_z is bending section coefficient of section $b-b$, the calculation equation is $\pi d^3/32 \approx 0.1d^3$, m^4 ; d is the diameter of stem $b-b$ section, m; F_s is the shear force generated on section $b-b$ used as a variable to analyze the fracture point in this study, N; S_z^* is static moment of the area under the chord parallel to the neutral axis at the point of over shear stress to the neutral axis, m^3 ; I_z is moment of inertia of the neutral axis of the entire cross-section, circular cross-section can be calculated by $\pi d^4/64$, m^4 .

According to the above analysis, if the torsional process before fracture always satisfies the tangential balance condition $\sum F_\tau = 0$ and moment balance equation $\sum M_b = 0$, at any time, then.

$$F_s = F_T \tag{3}$$

$$M_b = M_T \frac{L_{CB}}{L_{CF}} \tag{4}$$

where, F_T is the external pressure acting on the fruit surface at a certain height, and the direction is always tangent to the torsion radius. In this study, the breaking torque can be measured by the torque sensor through the test, and then converted to its value. In this study, it is considered as a force of constant magnitude, N; M_T is the breaking torque value measured by external motor output and torque sensor connected, with O_T point as the turning center and L_{CF} as the radius, N·m; L_{CB} is the distance between the breaking point and the fruit action point, namely, the value of $|h_C + h_B|$, is to be measured, mm; L_{CF} is the torsional radius, and in this study it is a variable factor, namely, the value of $|h_C + h_F|$, mm.

As shown in Equation (4), in order to ensure that the position of b - b section can be measured intuitively in subsequent tests, the initial set rotation axis point is lower than the fracture section, namely, $L_{CF} \geq L_{CB}$. The value M_T will be greater than the actual breaking moment. Therefore, it is necessary to obtain the fracture height of section b - b through multiple tests, and gradually adjust the

position of the point O_T until $h_B \approx h_F$ (or $L_{CF} \approx L_{CB}$), and the measured value M_T can be considered as approximately equal to M_b .

In order to obtain the influence law of the fruit-stem clamping height h_C and stem-stalk fixation distance h_F on the stress of the broken section of the stem, preliminary set $F_S=1$ N, $d=0.029$ m, and combine Equations (1)-(4), then the following equation can be obtained.

$$\begin{cases} \sigma_b = 0.42 \times (h_C + h_F) \\ \tau_b = \frac{6.4 \times 10^{-4}}{h_C + h_F} \end{cases} \tag{5}$$

Input Equation (5) into Origin to generate response surfaces of section normal stress and shear stress respectively. As shown in Figure 5, the fruit stem clamping height h_C has a greater impact on section normal stress σ_b , and the greater the clamping height, the greater the normal stress; The fixation spacing h_F between stems and stalks has a greater impact on the shear stress τ_b of the section, and the smaller the fixation spacing is, the greater the shear stress is. Therefore, it can be found through analysis, if the clamping point of the fruit is maximized ($h_C \rightarrow h_{Cmax}$, i.e., it is clamped at the top of the fruit or the hard area near the junction of the fruit crown), meanwhile, minimize the fixation spacing between stems and stalks ($h_C \rightarrow 0$, that is, the area near the bottom of the fruit), it can theoretically achieve fast and efficient fruit stem fracture separation.

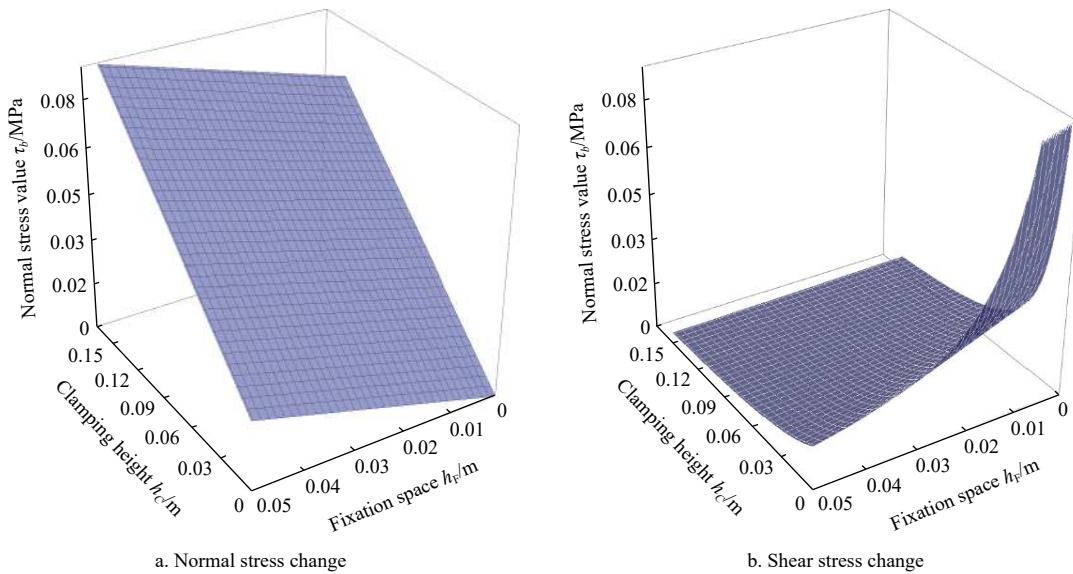


Figure 5 Curved surface diagram of the influence law on the stress in the broken section of the stem with h_C and h_F

On the other hand, in order to more accurately obtain the critical fracture angle at the instant of fruit stem separation, it is assumed that a certain deflection curve will be generated in the area near the fracture section during bending, and the rotation angle equation can be obtained by integrating the differential equation of the deflection curve, as follows.

$$\theta_s = \frac{\int M_b(z) dz + C}{EI_z} = -\frac{M_b L_{CB}}{2E_{co} I_z} \tag{6}$$

where, θ_s is the angle of fruit breaking, that is, the angle between the fruit axis and the vertical direction at the critical moment of fruit stem separation, and the angle between the normal line direction and the z axis (vertical direction) on the b - b section at the breaking moment, rad; E_{co} is the elastic modulus of the material near the fruit stem fracture section, MPa.

For the unknown quantity E_{co} in Equation (6) in this study, the

specific value shall be obtained by reverse calibration through the measured value of torque M_b , torsion radius L_{CB} and rotation angle θ_s at the moment of fracture. The results do not represent the resilience of the stem, only reflect the physical characteristics of the fruit stem connection.

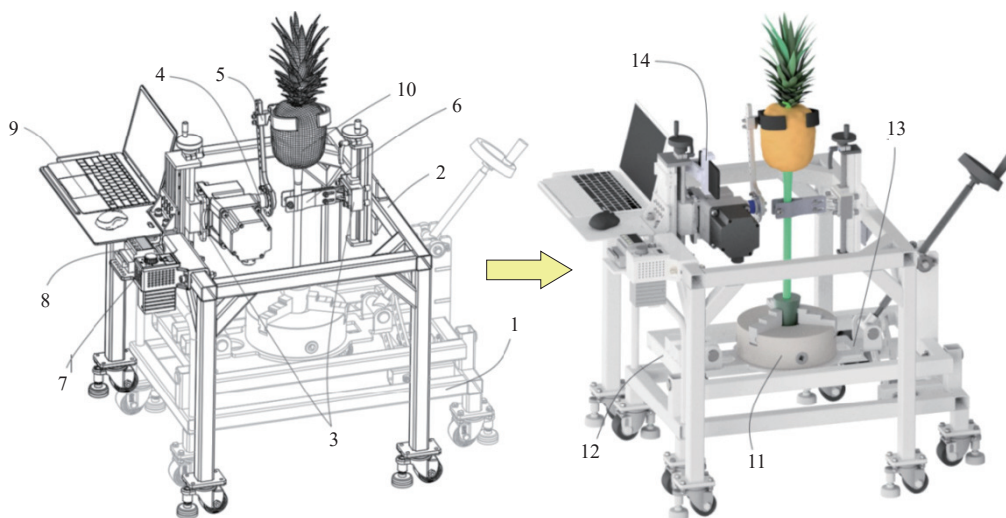
2.3 Conditions and methods of experiments

2.3.1 Development of experiment equipment

In order to ensure accuracy, it is necessary to build a plant experiment platform similar to the actual environment for testing. Aiming at the growth posture of pineapple standing in the field, a plant fixation test platform for simulating the growth posture of pineapple in the field (referred to as plant fixation platform)^[10] and a torque measurement test equipment for pineapple fruit stem bending separation (referred to as torque measurement equipment)^[21] have been designed and developed. The test can be carried out only when

the above two devices are used together, as shown in Figure 6. The plant fixation platform mainly includes the stem fixation chuck, the roll angle adjustment device and the pitch angle adjustment device, which are mainly used to simulate the overall root fixation state of the plants, and can realize the setting and adjustment of a variety of

lodging and tilting postures. The torque measuring equipment mainly comprises a moving frame, a linear sliding platform module, a torque sensor, a torsion arm, a straw fixing clip, a speed controller, a transmitter, a portable computer and a camera module fixing frame.



1. Plant fixation platform 2. Mobile frame 3. Linear sliding table module 4. Torque sensor 5. Torsion arm 6. Straw fixing clip 7. Speed controller 8. Transmitter 9. Portable computer 10. Single pineapple plant 11. Straw fixation chuck 12. Pitch angle adjustment device 13. Roll angle adjustment device 14. Camera module holder

Figure 6 Structural diagram of combined experiment equipment

2.3.2 Experimental principle and implementation mode

When measuring the critical torque of pineapple fruit-stem fracture, it is necessary to fix a complete single sample of pineapple plant on the plant fixation platform or other fixtures that can simulate the root fixation in the field to ensure that the overall pineapple plant is similar to the growth posture in the field. Next, adjust the pineapple plant monomer to the “hollow area” inside the mobile platform. According to the requirements of the experiment design, first turn the rotary handle above the linear slide module in the clamping part, adjust the stem fixation clip to the required appropriate height, and then lock the stem, and then turn the rotary handle above the linear slide module in the torsion part, adjust the axial position of the torque sensor to the coaxial position close to the clamping point, and then fit the fruit fixation clip on the surface of the pineapple fruit to be measured, and adjust it through multiple

holes on the torsion arm. And then rotate the torsion arm to an angle close to the collinear with the stalk. Finally, electrify the equipment and the portable computer, start the collection state of the upper computer software, adjust the speed controller to a certain value, start the motor to rotate until the pineapple fruit and stem are completely broken and separated, stop the motor, and end the data collection state, then the result data can be exported and the maximum torque value of the broken pineapple can be viewed.

In order to observe and analyze the moment of fracture action, the camera fixation seat can be buckled on the upper two ends of the straightline sliding platform module, and a micro camera or smart phone can be installed. Through high-speed photography and slow motion inspection or marking, the fruit fracture angle or other important information can be further obtained. The object after development, molding and assembly is shown in Figure 7.

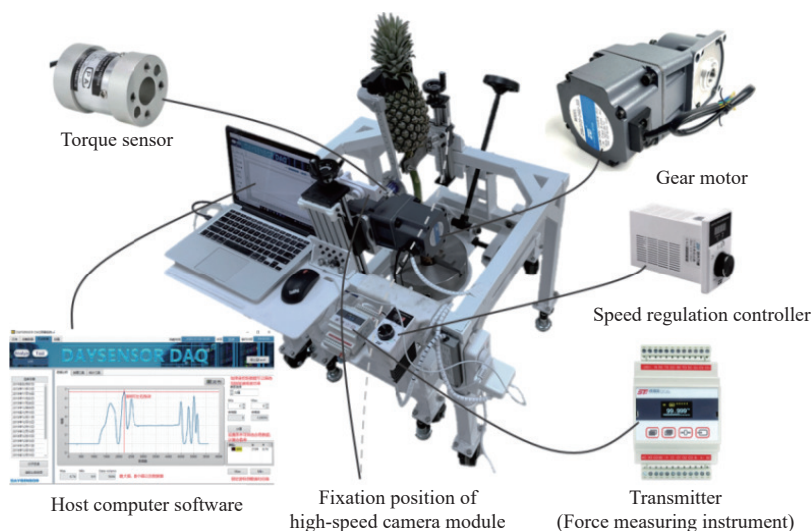


Figure 7 Physical objects of combined experiment equipment

2.3.3 Experimental object and material treatment

The pineapple plants for experiment were selected from the representative Bali varieties in South China. The sample was produced in Ganhu Village, Gaopo Township, Qujie Town, Xuwen County, Zhanjiang City, Guangdong Province. 50 complete plants of similar size were selected with a maturity stage of C0-C2 and free of pests and diseases and canker, as shown in Figure 8. Healthy and mature plants generally have dentate and thick leaves (about 40 leaves per plant). To facilitate the experiment and observation, cut and peel all its leaves; However, in the process of peeling leaves, it

is found that after the fruit enters the mature stage, several supporting bud seedlings are generally grown from the stem at the fruit stem connection part, and the fruit is wrapped around. Whether it will cause certain hindrance to the fracture and separation of fruit and stem is still an unknown problem. Therefore, considering the accuracy of this study, the plants after peeling leaves are divided into two categories, one is the monomer that retains supporting buds, the other is the monomer that removes supporting buds, The influence degree will be determined through comparison experiment in the future.

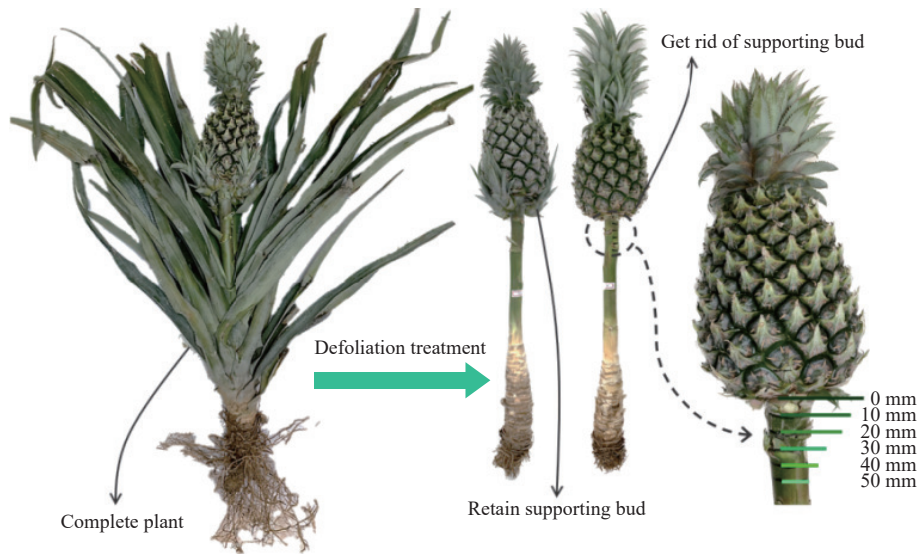


Figure 8 Schematic diagram of plant monomer treatment, classification and labeling

According to the above analysis of the results of the mechanical model, on the defoliated plant, take the pineapple stem (O_S point in Figure 3) as the starting zero point, take the spacing of 10mm as the unit length, and use a black marker to mark its scale value, so as to accurately fix the different height positions of the stem and ensure the accuracy of the experiment results.

2.3.4 Experimental conditions and operating parameters

The experiment was conducted in Key Laboratory of the South China Modern Agricultural Intelligent Equipment of the Ministry of Agriculture and Rural Affairs (No. 1, Fenghuangsi Road, Jiulong Town, Huangpu District, Guangzhou, China). The specifications and parameters of the selected motor and torque sensor are listed in Table 1, where the real-time torque of the motor output shaft is

$$M'_t = \frac{9549P_n}{n_i} \quad (7)$$

where, M'_t is the external force torque applied on the fruit and also the output torque of the motor shaft, $N \cdot m$; P_n is the rated power transmitted by the external motor shaft, kW, The rated power of the motor in this experiment is 0.2 kW; n is the speed of external motor output shaft, r/min, and the speed regulation range of this experiment is from 0 to 3000 r/min; i is the reduction ratio of motor transmission box, which is 1:100, and the maximum torque that the reduction box can withstand is 40 $N \cdot m$.

According to Equation (7), when the motor output shaft is at the maximum speed (30 r/min), the realtime output torque value is the minimum (about 64 $N \cdot m$), and the maximum output torque is only the limit that the gearbox can withstand, that is, 40 $N \cdot m$, so the real-time output torque within the speed regulation range is always 40 $N \cdot m$. It can be seen that the motor speed in this experiment has no effect on the result of breaking torque of fruit stem, and the

initial constant speed selected for the experiment is 20 r/min. The torque sensor is DYJN-104 of Chinese DAYSENSOR brand, and the upper computer is its supporting DAQ measurement system. And the specific parameters and specifications of other auxiliary components, controllers and related devices are listed in Table 1.

Table 1 Experimental conditions and parameter specification

Items	Parameter category	specifications
Gear motor	Rated power	300 W
	Speed regulation range	0-3000 r·min ⁻¹
	Reduction ratio	1:300
	Maximum torsion	40 N·m
Torque sensor	Measurement range	0-30
	Range of the handle height	0-200 mm
Linear module	Range of rear mounting hole table	0-150
Measurement system	Data export format	.xls

3 Scheme design of experiment

It can be known from the above fruit fracture mechanism that setting the fruit clamping point to the maximum position, namely, increasing the action torque, can obviously improve the fracture efficiency of fruit and stem. Therefore, in consideration of the similar height of the fruit and stem of the sample, the fruit clamping height is taken as a more appropriate fixation value (that is, the clamping point is near the junction of the fruit crown). On the other hand, it also can be known from the analysis mechanical behavior and stress that the closer the distance between the torsion center and the connection of the fruit stem, the greater the effective effect of the bending moment to produce fracture. Therefore, the rotation center of the torsion arm is also adjusted and fixation close to the

connection of the fruit stem (that is, near the O_S point). So far, the fixation torsion arm is 200 mm (that is, $h_C=150$ mm, $h'_F=50$ mm, wherein h'_F is the distance between the rotation center and the fruit-stem connecting point O_S of the fruit and stem). In the following experiment, the fracture position, torque size, and fracture angle of the fruit during bending and torsion should be studied and analyzed.

3.1 Grouping design of single factor

First of all, 40 plants without supporting buds and 10 plants with supporting buds were allocated into two groups, in which 10 plants without supporting buds and 10 plants with supporting buds were selected for large-scale comparison experiment, and the remaining 30 plants were equally divided into 15 plants in two parts, one of which was divided into five groups, 3 plants in each group were selected for small-scale experiment, and the other part was selected as the candidate for validation optimization experiment.

The above large-scale experiment method is specifically as follows: take the fixation spacing between stems and stalks as a factor, and the torque value measured by the fruit fracture as an indicator, set five horizontal values with large spacing evenly on the stem, and conduct twice for each horizontal to record the output results of the whole process.

The above small-scale experiment method is specifically as follows: set five horizontal values with smaller spacing near the fruit stem connection point, conduct three times at each horizontal, and record the output results of the whole process with the breaking torque value M'_T and the fruit breaking angle θ_S as indicators. The specific experiment scheme is listed in Table 2.

Table 2 Experiment design of single factor

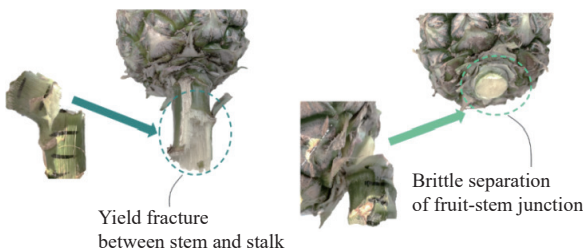
Factor	fixation spacing between stems and stalks h_{FIs} /mm	fixation spacing between stems and stalks h_{Fss} /mm
	50	10
level	100	20
value	150	30
	200	40
	250	50

*Note: In the table, h_{FIs} is the fixation spacing of stems and stalks set under largescale conditions, h_{Fss} is the fixation spacing of stems and stalks set under small-scale conditions.

4 Results and analysis

4.1 Large scale experiment results

The experiment results are shown in Figure 9. When the stem-stalk fixation distance is 50 mm, the breaking torques M'_T of the two experiments are 2.78 N·m and 3.06 N·m respectively. With the increase of the fixation distance, the torque required for fruit



Note: h_{FIs1} and h_{FIs2} in the figure are fixation spacing values between stem and stalk of two repeated tests.

Figure 9 Variation curve of torque in large scale experiment

breaking increase accordingly. When the stem-stalk fixation distance is 200-250 mm, the breaking torque reaches its maximum

(about 10 N·m), which is consistent with the above theoretical analysis.

On the other hand, as shown in Figure 10, when observing the position of the fruit-stem fracture section, it was found that when the stem-stalk fixation distance was greater than 50 mm, the fracture point mostly occurred on the lower stem section (that is, the fracture section was 60 mm away from the junction of fruit and stem), and it exceeded the bending strength of the stem and caused yield and fracture. When the stem-stalk fixation distance was less than 50 mm, the fracture points are all near the junction of the fruit and stem (that is, the fracture section is within 9mm from the junction of the fruit stem), and they are brittle separation. The main reason for the above results is that with the increase of the fixation distance, even though the torsion center remains near the junction of fruit and stem, different sections in the area below the torsion center will also generate continuous normal stress, thus generating large elastic deformation, and the maximum bending moment section will occur at the length of the radius of gyration below the junction of fruit and stem. Therefore, the increase in the stem-stalk fixation distance is equivalent to adding bending moments under the stems that do not contribute to the fracture of fruit and stems, and during the bending process, the stress yield limit must be reached at a certain section of the stems below the junction of fruit and stem, thus causing destructive fracture of the stems. In addition, the comparative experiment results in the large-scale experiment show that the influence of the supporting buds and the non-supporting buds on the fracture difficulty can be almost ignored. The supporting buds in the picking season are small in size and have no obvious effect on the fruit wrapping. The bud seedlings are mainly attached by the side wall of the stem and grow up along the fruit. Observation shows that the more the planting points, the more the convex and concave structures at the junction of the fruit and stem, and the more brittle fracture occurs.

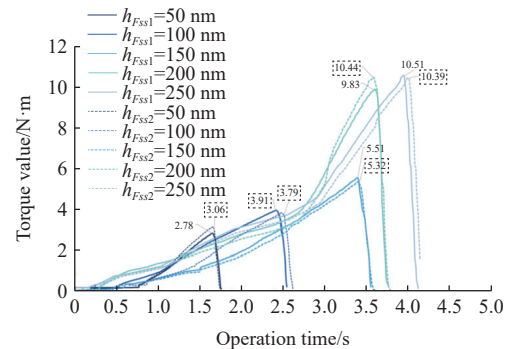


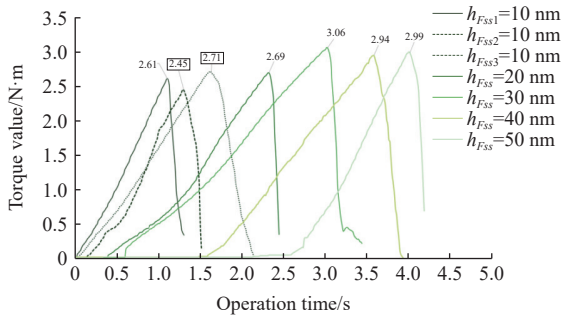
Figure 10 Different fractures and separations of pineapple and stem

4.2 Small scale experiment results

The experiment results are similar to those of large-scale experiments, and there is no obvious difference between the results with or without stipules. In order to express them clearly and intuitively in the paper, some test data are selected for analysis, as shown in Figure 11. When the stem-stalk fixation distance is within 50 mm, according to the measured data, the breaking torque M'_T will increase slightly with the increase of stem-stalk fixation distance, which is mostly distributed in the range of 2.61-3.06 N·m. In addition, all the fruits in the experiment were separated brittlely, and the distance between the fracture section and the junction of the fruit and stem was within 7 mm.

4.3 Fruit fracture and the extraction of separation angle

Select the experimental group of plants without supporting



*Note: h_{Fss1} , h_{Fss2} and h_{Fss3} in the figure are fixation distance values between stems and stalks in three repeated tests.

Figure 11 Torque variation curve of small-scale experiment

buds and with stem-stalk fixation distance less than 50 mm, export the data of slow motion video stream recorded in the process of experiment, extract the instantaneous start frame of fracture and the end frame after complete separation respectively, as shown in Figure 12a and Figure 12c. After grayscale conversion, use the canny operator to detect the edges, and further match and mark the fruit centerline and stem centerline based on the recognized contour, and measure the included angle value of the two, as shown in Figure 13.

The measurement results are shown in Figure 14. There are five

horizontals when the stem-stalk fixation distance is within 50 mm and three experiments are conducted at each horizontal. In total, there are fifteen groups of experiments. The results show that when the stem-stalk fixation distance is small (the stem-stalk fixation distance is within 40 mm), the range of instantaneous angle of fracture occurrence (referred to as the initial angle for short) is $[12.7^\circ, 15.4^\circ]$, and the range of instantaneous termination angle of complete separation (referred to as the termination angle for short) is $[94.8^\circ, 100.5^\circ]$. With the increase of the stem-stalk fixation distance, the initial angle and termination angle both increase to a certain extent. When the stem-stalk fixation distance is 50 mm, the maximum initial angle and termination angle can reach 19.2° and 103.4° . The reason for this result may be that with the increase of the stem-stalk fixation distance, the maximum bending moment point of the stem shifts downward during bending, and the stem between the fixation point and the fruit stem connection point has some flexible deformation. Therefore, parts of rotation angle at the upper end of the stem make the increase of the total angles of fruit fracture. According to the statistics of the difference between the termination angle and the initial angle in each group of experiment data, they are evenly distributed in the range $[82.9^\circ, 87.5^\circ]$, so it can be preliminarily identified as the travel range of the fracture separation angle of pineapple fruit and stem.

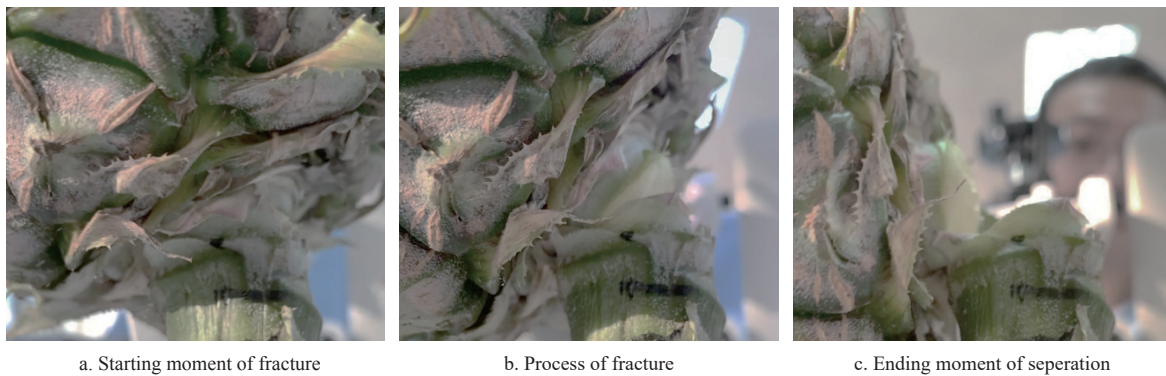
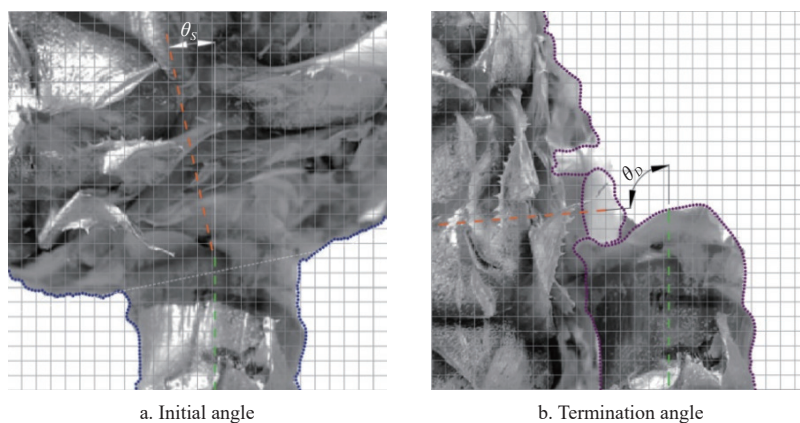


Figure 12 Recording process of high speed camera



*Note: The orange line in the figure is the median line of pineapple fruit. The green line is the center line of the stem, which is approximately vertical in this paper. θ_s is the instantaneous initial fruit fracture angle. θ_d is the instantaneous termination angle of complete separation of fruit and stem. Blue and purple dotted lines are the recognized edge contour lines.

Figure 13 Angle extraction and marking process

4.4 Optimization design and verification experiment

In order to better realize the accurate screening of the influence range of factors, D optimal design method is selected for the quadratic random experiment on the basis of the above experiment results, taking the fracture torque and fracture initial angle as two

response indicator values, as Y_1 and Y_2 . The factor levels and test results are listed in Table 3.

The variance analysis of each response value in Table 3, as shown in Table 4, shows that the value test results of R^2 and P under the linear model are within the reasonable range under the response

value Y_1 , and the test results of the linear and quadratic models are within the reasonable range under the response value Y_2 , as shown in Table 5. The reliability of the variance sources in the linear model has been verified^[22], and the fitting results of the regression model are as follows.

$$Y_1 = 2.368 + 0.019X \quad (8)$$

$$Y_2 = 15.016 - 0.217X + 0.0052X^2 \quad (9)$$

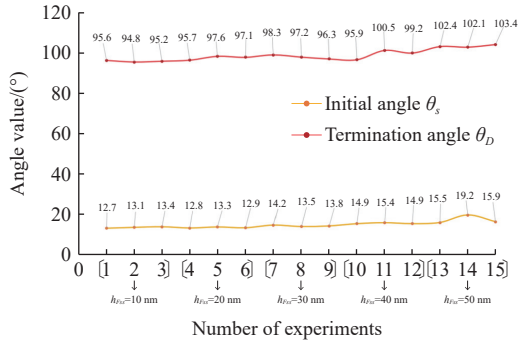


Figure 14 Experimental results of fracture and separation angle

Table 3 Factor levels and indicators.

Number	Factor	Indicators	
	X	Y_1	Y_2
1	10	2.73	13.4
2	10	2.55	13.5
3	10	2.62	13.7
4	15	2.43	12.2
5	20	2.59	12.5
6	25	2.92	13.1
7	30	2.99	13.4
8	36	2.98	14.1
9	43	3.34	15.3
10	50	3.02	18.1
11	50	3.44	16.4
12	50	3.13	17.1
13	50	3.57	16.9

*Note: In the table, X is the unitless value of stem-stalk fixation distance; Y_1 is the unitless value of breaking torque; Y_2 is the unitless value of initial angle of fracture.

Table 4 Factor levels and indicators

Model	Y_1				Y_2			
	p_1	p_2	R^2_{adj}	R^2_{pred}	p_1	p_2	R^2_{adj}	R^2_{pred}
Linear model	< 0.0001	0.7734	0.7502	0.6669	< 0.0001	0.0447	0.7223	0.6419
Square	0.8032	0.6952	0.727	0.6283	< 0.0001	0.7693	0.9373	0.9145
Cube	0.2357	0.7615	0.7428	0.625	0.4177	0.75	0.9355	0.91
Quartic	0.5293	0.6974	0.7255	0.4768	0.1698	0.9371	0.9435	0.9225

*Note: p_1 is the value of p continuous variables in the table. p_2 is the value p of model mismatch detection. R^2_{adj} is adjusted variance for fitting model. R^2_{pred} is the prediction variance of the fitting model.

Table 5 Continuous test results of F for selected models

Response value	Model	Sum of Squares	Degrees of freedom	Mean square	F-value	p-value
Y_1	X	1.18	1	1.18	37.03	< 0.0001
	X^2	29.4	1	29.4	124.74	< 0.0001
Y_2	X	9.12	1	9.12	38.7	< 0.0001
	X^2					

Considering the high efficiency demand of actual pineapple harvesting in the field, it is generally expected that the external torque and action amplitude required for fruit fracture and separation are minimal as far as possible. Therefore, based on the above results, the constraint conditions of the optimization objective function are set as follows.

$$\begin{cases} \min Y_1; \min Y_2 \\ \text{s.t.} \begin{cases} 10 \leq X \leq 50 \\ 0 \leq Y_1 \leq 3 \\ 0 \leq Y_2 \leq 14 \end{cases} \end{cases} \quad (10)$$

Introduce Equation (8) and Equation (9) into the Origin, merge the two response values into a chart, and further delimit the range of the optimal solution according to the constraint conditions, as shown in Figure 15, the selected range is $X \in [12, 30]$. Set the importance of Y_1 is “+++”, and the importance of Y_2 is “+++++” in Design Expert, the optimal solution is $X = 14.7$, at this time $Y_1 = 2.64$, $Y_2 = 12.95$, that is, when the stem-stalk fixation distance is 14.7 mm, the predicted breaking torque is about 2.64 N·m and the initial angle of fracture is about 12.95°.

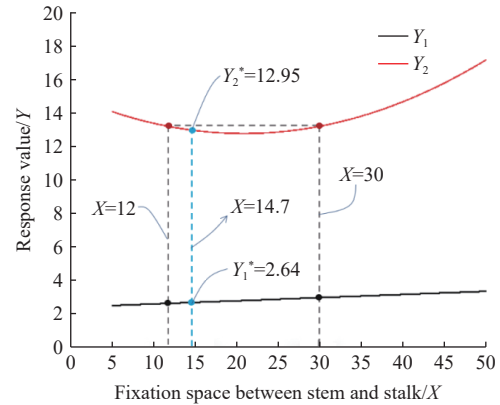


Figure 15 Optimal solution range of fitting results

In order to verify the validity of the regression model, the plants without stipules that are similar to the experiment samples in the stem size, fruit diameter and height were selected for the validation experiment. Adjust the stem-stalk fixation distance to 15mm, and take the average value of the breaking torque and the breaking initial angle measured in the repeated three experiments. The result is $\bar{M}_b = 2.76$ N·m, $\bar{\theta}_s = 13.8$ N·m, which is very close to the optimization result, with the maximum error of about 13.1%. So far, we can think that the regression model has certain correctness, it can provide reliable reference for subsequent research and design.

5 Analysis of physical characteristics

5.1 Discussion on section stress

Equation (2) in Section 2 above shows that when brittle fracture occurs, either normal stress or shear stress of the section at the junction of fruit and stem reach the strength limit first. Therefore, the measured torque value and stem-stalk fixation distance can be substituted to Equation (3) and Equation (4) to calculate the corresponding section bending moment value and shear force value, and the section stress value can be further obtained accordingly.

The mean values of the actual bending moment and shear force at the fracture section of pineapple fruit and stem can be obtained by selecting the optimization experiment results with the stem-stalk fixation distance within 50 mm. The calculation equation is as follows

$$\bar{M}_b = \frac{\sum_{i=1}^N \left[M_T(i) \times \frac{L'_{CB}(i)}{L_{CF}(i)} \right]}{N} \quad (11)$$

$$\bar{F}_s = \frac{\sum_{i=1}^N \left[\frac{M_T(i)}{L_{CF}(i)} \right]}{N} \quad (12)$$

where, $L'_{CB}(i)$ is the sum of the distance h_B between the fracture section and the fixation height h_C of the fruit measured in each group of experiments, mm; i is the serial number of the test, $i = 1, 2, 3, 4$; N is the number of samples in the experiment group. The total number of samples in this experiment is 13 groups.

Through calculation, the range of bending moment value required for the fracture of fruit and stem is 1.88-2.77 N·m and its mean value is $\bar{M}_b = 2.29$ N·m, the mean value of shear force is $\bar{F}_s = 14.73$ N. Substitute them to obtain the mean value of normal stress is $\bar{\sigma}_b = 0.94$ MPa and the mean value of shear stress is $\bar{\tau}_b = 0.03$ MPa in the critical state of fracture. The maximum value of normal stress is $\bar{\sigma}_{b\max} = 1.14$ MPa, and the maximum value of shear stress is $\bar{\tau}_{b\max} = 0.036$ MPa. Although the result shows that the normal stress of the section is greater than the shear stress. For the pineapple plant, the mechanical behavior of the whole bending fracture process is to act on the upper end of the fruit, and the fruit whose diameter is much larger than the stem is also involved in overcoming the bending moment in its process. Considering that the junction between the fruit and the stem is a mutation area of the section, its shear stress and normal stress have a great probability of reaching the strength limit at the junction at the same time. Therefore, in combination with the subsequent uniaxial tensile and pure shear experiments, we can obtain the yield limit to accurately determine which stress plays a major role in fracture^[23]. The test results in this paper can be used as the data source and reference for subsequent research and analysis.

5.2 Calibration of elastic modulus

In the critical state of instant fracture, the fruit and stem will have a certain degree of flexible deformation and angle change. Equation (6) in Section 2 above shows that the estimated range of elastic modulus of materials near the fracture section of the fruit stem can be further inversely calculated according to the change range of the fracture angle θ_S of the fruit in the experiment results^[24]. The calculation equation is as follows.

$$E_{co} \in \left[\left[-\frac{\bar{M}_b \bar{L}'_{CB}}{2\theta_{S\max} I_z}, -\frac{\bar{M}_b \bar{L}'_{CB}}{2\theta_{S\min} I_z} \right] \right] \quad (13)$$

where, \bar{L}'_{CB} is the mean distance between the breaking point and the fruit action point, mm, the mean value is obtained by summing the distance h_B between the breaking section measured in each experiment and the fixation height h_C of the fruit. According to the above experiment results, the mean distance between the breaking section and the junction of fruit and stem is 0.0051 m, that is, $\bar{L}'_{CB} = 0.155$ m. $\theta_{S\max}$ is the maximum experiment value of fruit breaking angle, the above result is 18.1°, that is, 0.316 rad. $\theta_{S\min}$ is the minimum experiment value of fruit breaking angle, the above result is 12.2°, that is, 0.213 rad. I_z is the moment of inertia of the broken cross section of the stem to the neutral axis, and the section is like a circle, it is calculated according to $\pi \bar{d}^4/64$ ($\bar{d} \approx 0.029$ m). In this paper, it is taken as 3.47×10^{-8} m⁴.

The elastic modulus of junction of pineapple fruit and stem, that is E_{co} is about in range 16.1-23.9 MPa, it can be obtained by inverse solution of Equation (13), which can provide the basis for

setting material parameters for subsequent simulation modeling of pineapple fruit and stem.

6 Discussion and conclusions

In this study, taking single pineapple plant as the research object, we completed the sampling statistics of physical characteristics and structural dimensions, in combination with the agronomic requirements of field management through onsite investigation, and based on the current “breakoff” method of harvesting, and analyzed the main factors affecting the fracture of fruit and stem and separation effect. Through mechanical behavior analysis and mathematical model creation, the best working conditions affecting the fruit fracture and separation were clarified, that is, maximize the holding point of fruit, and minimize the stem-stalk fixation distance, which can theoretically achieve fast and efficient fracture separation of fruit and stem.

On the premise of clarifying the mechanism of fracture of fruit and stem, the “pineapple plant fixation platform” and “fruitstem bending separation torque experiment equipment” have been independently developed. Based on the previous theoretical research, the single factor experiment of scale has been carried out, and the optimization verification experiment has been completed. The results show that the wrapping effect of the fruit with or without supporting buds can be ignored, and the impact on the fracture difficulty is small. With the constant increase of stem-stalk fixation distance, the torque required for fruit fracture and the fracture initial angle increase accordingly. When stem-stalk fixation distance is less than 50 mm, the probability of brittle fracture and complete separation is extremely high. The average distance between the fracture section and the junction of fruit and stem is about 5 mm. The range of bending moment required for fracture of fruit and stem is 1.88-2.77 N·m, the range of fracture initial angle is 12.2°-18.1°, and the angle stroke during separation is 82.9°-87.5°. According to the measurement results of the initial angle of fracture between the fruit and the stem, the elastic modulus of the junction of fruit and stem was estimated to be within the range of 16.1-23.9 MPa.

Through the analysis of the data in optimized experiment, we obtain the best conditions for the separation of fruit and stem, that is, when the stem-stalk fixation distance is 14.7 mm (can be rounded to 15 mm), the predicted breaking torque is about 2.64 N·m. The initial angle of fracture is about 12.95°, and the verification experiment results show that the breaking torque is about 2.76 N·m. The fracture initial angle is about 13.8°, and the maximum error is about 13.1%.

In conclusion, through the experimental research and result analysis in this paper, we can further accurately learn the pineapple fruit-stem fracture mechanism. The conclusion provides a research basis for the best method and means of fruit harvesting, and can provide an important design basis for the research and development of pineapple field harvesting robots and harvesting equipment in the future.

Acknowledgements

This research was financially supported by the Construction Project of PhD Workstation in Guangdong Province (Guangdong Provincial Financial Administration [2020] No. 122) and the Special Fund for Rural Vitalization Strategy in Guangdong Province (Guangdong Provincial Financial Administration [2022] No. 92). The authors also acknowledge the reviewers for their constructive suggestions on improving this manuscript.

[References]

- [1] CIGR Handbook of Agricultural Engineering, Vol. III Plant Production Engineering, Chapter 1 Machines for Crop Production, Parts 1.1. 1–1.1. 4 Human-Powered Tools and Machines. pp.1–22. Available online: <https://elibrary.asabe.org/abstract.asp?aid=36337> Accessed on [2022-05-01]
- [2] Goren R. Anatomical, physiological, and hormonal aspects of abscission in citrus. *Hortic. Rev.*, 2010; 15: 145–182.
- [3] Liu J Z, Li P, Li Z G, Mao H P. Experimental study on mechanical properties of tomatoes for robotic harvesting. *Transactions of the CSAE*, 2008; 24(12): 66–70.
- [4] Liu T H, Ehsani R, Toudeshki A, Zou X J, Wang H J. Experimental study of vibrational acceleration spread and comparison using three citrus canopy shaker shaking tines. *Shock and Vibration*, 2017; 2017: 1–9.
- [5] Bhat K, Chayalakshmi C L. Microcontroller-based semiautomated pineapple harvesting system. In *International Conference on Mobile Computing and Sustainable Informatics*; Springer, Cham, Switzerland, 2020; pp.383–392.
- [6] Liu J. Analysis on concentration and competitiveness of Xuwen pineapple industrial cluster. *Chinese Journal of Tropical Agriculture*, 2022; 42(9): 92–98.
- [7] Li M T, Chen H, Huang X H, Zhang Z Z, He L. Current status and development analysis of entire field mechanization of pineapple industry. *International Agricultural Engineering Journal*, 2019; 28(2): 46–54.
- [8] Liu T H, Liu W, Zeng T J, Qi L, Zhao W F, Cheng Y F, et al. Working principle and design of the multi-flexible fingered roller pineapple harvesting mechanism. *Transactions of the CSAE*, 2022; 38(8): 21–26. (in Chinese)
- [9] Liu T H, Liu W, Zeng T J, Cheng Y F, Zheng Y, Qiu J. A multi-flexible-fingered roller pineapple harvesting mechanism. *Agriculture*, 2022; 12: 1175.
- [10] Gan L, Li M T, Wang B B, He L, Chen Z W, Yue D D, et al. A plant fixation test bench for simulating the growth posture of pineapple in the field. *China Patent*, CN 114009208 B, 2022.11. 29. (in Chinese)
- [11] Zhang J C. Optimization design and analysis of pineapple automatic picker. MS dissertation, Zhongkai University of Agricultural and Engineering, 2015. (in Chinese)
- [12] Zhang R H, Zhang Q, Qu J S, He K J, Wang Z W, Lu D X. Design and control of self-propelled pineapple flower induction machine with high gap. *Electromechanical Engineering Technology*, 2022; 51(6): 18–21.
- [13] Li B, Wang N, Wang M H, Li L. In-field pineapple recognition based on monocular vision. *Transactions of the CSAE*, 2010; 26(10): 345–349. (in Chinese)
- [14] He D J, Zhang L Z, Li X, Li P, Wang T J. Design of automatic pineapple harvesting machine based on binocular machine vision. *J. Anhui Agric. Sci.*, 2019; 47(13): 207–210. (in Chinese)
- [15] Jiang T, Guo A F, Cheng X B, Zhang D, Li Jin. Structural design and analysis of pineapple automatic picking-collecting machine. *Chinese Journal of Engineering Design*, 2019; 26(5): 577–586. (in Chinese)
- [16] Liu J, Peng Y, Faheem M. Experimental and theoretical analysis of fruit plucking patterns for robotic tomato harvesting. *Comput. Electron. in Agric.*, 2020; 173: 105330.
- [17] Burks T, Villegas F, Hannan M, Flood S, Sivaraman B, Subramanian V, et al. Engineering and horticultural aspects of robotic fruit harvesting: Opportunities and constraints. *Hort Technol.* 2005; 15: 79–87.
- [18] Roshanianfard A, Noguchi N. Pumpkin harvesting robotic end-effector. *Comput. Electron. in Agric.*, 2020; 174: 105503.
- [19] Zhang Z, Igathinathane C, Li J, Cen H, Lu Y, Flores P. Technology progress in mechanical harvest of fresh market apples. *Comput. Electron. in Agric.*, 2020; 175: 105606.
- [20] Ikram M M M, Mizuno R, Putri S P, Fukusaki E. Comparative metabolomics and sensory evaluation of pineapple (*Ananas comosus*) reveal the importance of ripening stage compared to cultivar. *J. Biosci. Bioeng.*, 2021; 132(6): 592–598.
- [21] Li M T, Yue D D, He L, Zhang X, Wang B B, Lu W Y, et al. A torque measurement test equipment for pineapple fruit stem bending separation. *Chinese Patent*, Publication No: 202211470234.3, 2022-11-22. (in Chinese)
- [22] Jones B, Good P. I-Optimal versus D-optimal split-plot response surface designs. *Journal of Quality Technology*, 2012; 44(2): 85–101.
- [23] Kumar R. *Strength of materials*. Taylor and Francis, 2022-01-10.
- [24] Gou L, Zhao M, Huang J J, Zhang B, Li T, Sun R. Bending Mechanical Properties of Stalk and Lodging-Resistance of Maize (*Zea mays* L.). *Acta Agronomica Sinica*, 2008; 34(4): 653–661. (in Chinese)